ARTICLE

OBC
www.rsc.org/obc

Cyclodextrin complexation of a stilbene and the self-assembly of a simple molecular device †

Julia S. Lock,[a] Bruce L. May,[a] Philip Clements,[a] Stephen F. Lincoln *[a] and Christopher J. Easton[b]

[a] *Department of Chemistry, University of Adelaide, Adelaide, SA 5005, Australia. E-mail: stephen.lincoln@adelaide.edu.au*

[b] *Research School of Chemistry, Australian National University, Canberra, ACT 0200, Australia*

Received 29th August 2003, Accepted 17th November 2003
First published as an Advance Article on the web 22nd December 2003

(*E*)-4-*tert*-Butyl-4′-oxystilbene, **1**$^-$, is thermally stable as the (*E*)-**1**$^-$ isomer but may be photoisomerized to the (*Z*)-**1**$^-$ isomer as shown by UV-vis and ^{1}H NMR studies in aqueous solution. When (*E*)-**1**$^-$ is complexed by αCD two inclusion isomers (includomers) form in which αCD assumes either of the two possible orientations about the axis of (*E*)-**1**$^-$ in αCD·(*E*)-**1**$^-$ for which ^{1}H NMR studies yield the parameters: k_1(298 K) = 12.3 ± 0.6 s^{-1}, $\Delta H_1^{\ddagger}$ = 94.3 ± 4.7 kJ mol^{-1}, $\Delta S_1^{\ddagger}$ = 92.0 ± 5.0 J K^{-1} mol^{-1}, and k_2(298 K) = 10.7 ± 0.5 s^{-1}, $\Delta H_2^{\ddagger}$ = 93.1 ± 4.7 kJ mol^{-1}, $\Delta S_2^{\ddagger}$ = 87.3 ± 5.0 J K^{-1} mol^{-1} for the minor and major includomers, respectively. The βCD·(*E*)-**1**$^-$ complex either forms a single includomer or its includomers interchange at the fast exchange limit of the ^{1}H NMR timescale. Complexation of **1**$^-$ by *N*-(6^A-deoxy-α-cyclodextrin-6^A-yl)-*N*′-(6^A-deoxy-β-cyclodextrin-6^A-yl)urea, **2**, results in the binary complexes **2**·(*E*)-**1**$^-$ in which both CD component annuli are occupied by (*E*)-**1**$^-$ and which exists exclusively in darkness and **2**·(*Z*)-**1**$^-$ in which only one CD component is occupied by (*Z*)-**1**$^-$ and exists exclusively in daylight at $\lambda \geq 300$ nm. Irradiation of solutions of the binary complexes at 300 and 355 nm results in photostationary states dominated by **2**·(*E*)-**1**$^-$ and **2**·(*Z*)-**1**$^-$, respectively. In the presence of 4-methylbenzoate, **4**$^-$, **2**·(*Z*)-**1**$^-$ forms the ternary complex **2**·(*Z*)-**1**$^-$·**4**$^-$ where **4**$^-$ occupies the second CD annulus. Interconversion occurs between **2**·(*Z*)-**1**$^-$·**4**$^-$ and **2**·(*E*)-**1**$^-$ + **4**$^-$ under the same conditions as for the binary complexes alone. Similar interactions occur in the presence of 4-methylphenolate and 4-methylphenylsulfonate. The two isomers of each of these systems represent different states of a molecular device, as do the analogous binary complexes of *N*,*N*-bis(6^A-deoxy-β-cyclodextrin-6^A-yl)urea, **3**, **3**·(*E*)-**1**$^-$ and **3**·(*Z*)-**1**$^-$, where the latter also forms a ternary complex with **4**$^-$.

Introduction

The inclusion of hydrophobic guests within the annuli of native and modified cyclodextrins has led to a wide range of complexes among which are enzyme mimics, polymers and rotaxanes.[1,2] The knowledge gained from these cyclodextrin complexes raises the possibility of constructing simple molecular devices, which may be switched between different states as has been done with other types of complexes.[3] Photoisomerization of a stilbene,[4] as occurs with (*E*)- and (*Z*)-4-*tert*-butyl-4′-oxystilbene, (*E*)-**1**$^-$ and (*Z*)-**1**$^-$, is potentially a convenient way of exercising such control. Accordingly, the complexes of thermally stable (*E*)-**1**$^-$ formed with α- and β-cyclodextrin (αCD and βCD), αCD·(*E*)-**1**$^-$ and βCD·(*E*)-**1**$^-$, have been studied in basic aqueous solution to provide insight into the effect of CD annular size on complexation as a prelude to characterizing the (*E*)-**1**$^-$ complexes of the urea linked CDs,[5,6] *N*-(6^A-deoxy-α-cyclodextrin-6^A-yl)-*N*′-(6^A-deoxy-β-cyclodextrin-6^A-yl)urea, **2**, and *N*,*N*-bis(6^A-deoxy-β-cyclodextrin-6^A-yl)-urea, **3** (Scheme 1). The binary complex, **2**·(*E*)-**1**$^-$, is found to isomerize to **2**·(*Z*)-**1**$^-$ photochemically which forms a ternary complex, **2**·(*Z*)-**1**$^-$·**4**$^-$, with 4-methylbenzoate, **4**$^-$, and also with 4-methylphenolate and 4-methylphenylsulfonate, whereas **2**·(*E*)-**1**$^-$ does not. The control of these processes both photochemically and also through a combined photochemical and thermal cycle is examined and reveals the operation of a simple molecular device. The analogous complexes of **3** behave similarly.

† Electronic Supplementary Information (ESI) available: NMR spectra. See http://www.rsc.org/suppdata/ob/b3/b310519a/

Results and discussion

The photoisomerization of 1$^-$

The water solubilities of 4-*tert*-butyl-4′-hydroxystilbene, **1**H, and its conjugate base, **1**$^-$, are extremely low. However, complexation of **1**$^-$ by a CD renders it sufficiently soluble for photochemical and NMR studies to be carried out. The synthetic product (see Experimental section) is (*E*)-**1**H and as a consequence the UV-visible spectrum of a freshly prepared basic aqueous solution of **2** and (*E*)-**1**H represents that of the **2**·(*E*)-**1**$^-$ complex (spectrum *a* in Fig. 1). On exposure of this solution to daylight for 2 h in a Pyrex vessel (which cuts out much of the light of $\lambda \leq 300$ nm) complete isomerization to **2**·(*Z*)-**1**$^-$ occurs (spectrum *d*) as indicated by ^{1}H NMR spectroscopy. Irradiation of this solution at 300 nm in a quartz cuvette for 2 h produces a photostationary equilibrium between **2**·(*E*)-**1**$^-$ and **2**·(*Z*)-**1**$^-$ (spectrum *b*). When this is followed by irradiation at 355 nm for 2 h a new photostationary equilibrium is reached between the two isomers (spectrum *c*). By alternately irradiating at 300 nm and 355 nm, alternation between the photostationary states characterized by spectra *b* and *c* occurs. Complete thermal isomerization of **2**·(*Z*)-**1**$^-$ in solution to **2**·(*E*)-**1**$^-$ occurs on warming at 340 K for 12 h in the dark. Similar spectral changes are observed in the αCD, βCD and **3** complexes, consistent with the isomerization process being little affected by the complexing CDs.

NMR studies of the complexation of (*E*)-1$^-$ by αCD and βCD

Both αCD and βCD greatly increase the solubility of (*E*)-**1**$^-$ in basic aqueous solution consistent with the formation of the

DOI: 10.1039/b310519a

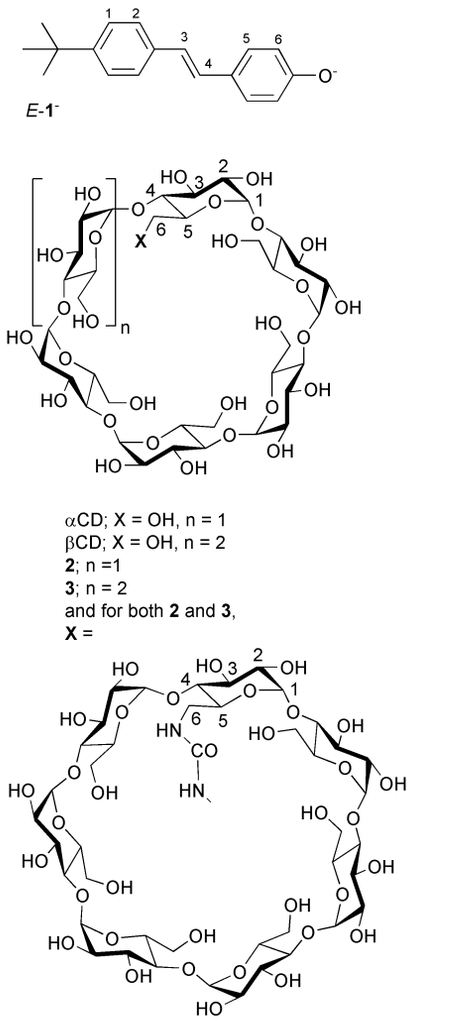

Scheme 1 The numbering shown for (E)-**1**$^-$ is used in the assignment of ^{1}H NMR resonances.

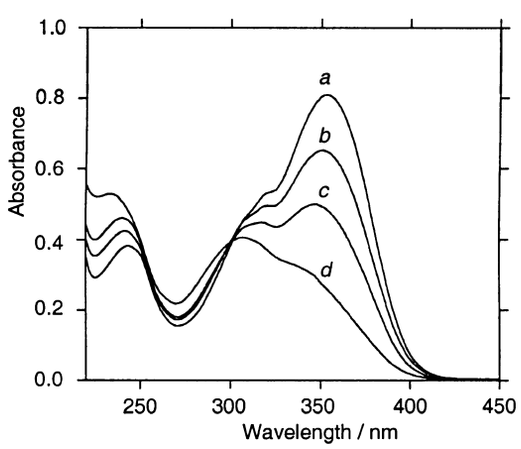

Fig. 1 The UV-visible spectral variation accompanying changes in the position of the equilibrium between (E)-**1**$^-$ and (Z)-**1**$^-$ for a solution in which total [(E)-**1**$^-$ and (Z)-**1**$^-$], [**2**] and [NaOH] = 2.5×10^{-5}, 2.6×10^{-5} and 1.2×10^{-4} mol dm^{-3}, respectively. *a* Initially prepared solution dominated by (E)-**1**$^-$; *d* after 2 h exposure to sunlight in a Pyrex vessel (Z)-**1**$^-$ dominates; *b* and *c* photostationary equilibria between (E)-**1**$^-$ and (Z)-**1**$^-$ after irradiation for 2 h at 300 nm and 355 nm, respectively.

complexes αCD·(E)-**1**$^-$ and βCD·*E*-**1**$^-$, respectively. To attain the higher concentration required for NMR spectroscopy, [NaOD] = 0.15 mol dm^{-3} is required which may indicate that it is necessary to deprotonate a hydroxy group of αCD·(E)-**1**$^-$ and βCD·(E)-**1**$^-$ (which is anticipated to have a $pK_a \geq 12$, on the basis that the pK_as of OH(2) and OH(3) are 12.33 for αCD) and thereby increase their solubilities.[7] (Similar NaOD concentrations were employed in studies of the systems of **2** and **3** discussed below.) The ^{1}H ROESY 600 MHz NMR spectrum of a D_2O solution in which $[\alpha CD]_{total}/[(E)\text{-}\mathbf{1}^-]_{total} = 3$ (the minimum ratio at which (E)-**1**$^-$ was completely solubilized at the concentration required) shows cross-peaks between the broadened doublet resonances of the (E)-**1**$^-$ aromatic protons and those of αCD, but no cross-peaks attributable to the *tert*-butyl protons of (E)-**1**$^-$ which exhibit two well resolved singlets (Figs. 2 and S1†). This is consistent with the formation of αCD inclusion complexes of (E)-**1**$^-$ where the annulus is positioned over the stilbene double bond and the *tert*-butyl protons of (E)-**1**$^-$ are too distant from the aliphatic protons of αCD for sufficiently strong dipolar interactions to generate cross-peaks between them. The simplest explanation of this is the formation of two isomeric αCD·(E)-**1**$^-$ inclusion complexes or includomers (Scheme 2). Such includomers produce two magnetic environments for the (E)-**1**$^-$ aromatic and vinylic protons through different interactions with the H3, H5 and H6 protons on the interior of the αCD annulus. The differing stereochemical arrangements of the primary and secondary hydroxy groups of αCD affect their interactions with the stilbene *tert*-butyl group of (E)-**1**$^-$ and probably its interaction with water and thereby produce two magnetic environments. While these individual interactions are weak their cumulative effects are sufficient to affect the magnetic environment of the *tert*-butyl group to give two resonances under slow includomer interchange conditions at 283 K.‡

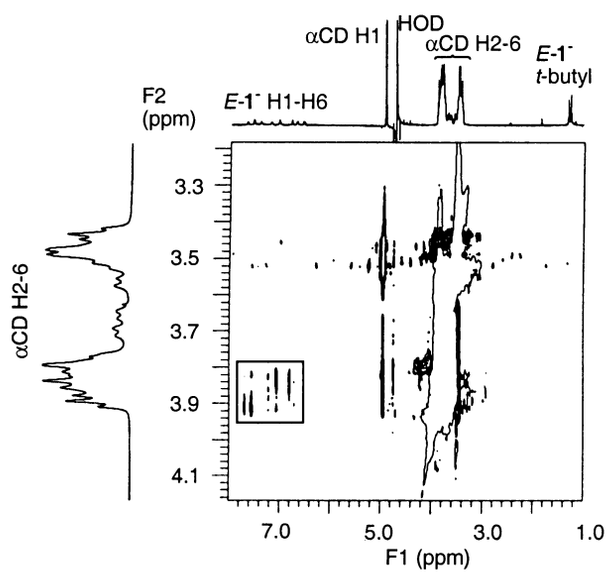

Fig. 2 ^{1}H 600 MHz ROESY NMR spectrum recorded at 298 K of a D_2O solution in which total [αCD], [(E)-**1**$^-$] and [NaOD] = 0.010, 0.0034 and 0.15 mol dm^{-3}, respectively. The cross-peaks enclosed in the rectangles arise from dipolar interactions between the protons indicated on the F1 and F2 axes.

In contrast, the ^{1}H ROESY NMR spectrum of a D_2O solution in which $[\beta CD]_{total}/[(E)\text{-}\mathbf{1}^-]_{total} = 1$ shows cross-peaks between resonances of the aromatic and *tert*-butyl protons of (E)-**1**$^-$ and those of βCD consistent with the formation of

‡ An alternative explanation for the complexed (E)-**1**$^-$ experiencing different magnetic environments is the formation of an $(\alpha CD)_2$·(E)-**1**$^-$ complex. Such a complex could exist as up to four includomers when the head-to-head, head-to-tail and tail-to-tail arrangements of the αCD pairs are taken into account. Molecular modelling indicates that each $(\alpha CD)_2$·(E)-**1**$^-$ should show ^{1}H ROESY NMR cross-peaks as a consequence of dipolar interactions of some of the H3, H5 and H6 protons on the interior of the αCD annulus with the *tert*-butyl protons of (E)-**1**$^-$. Because such cross-peaks are not observed $(\alpha CD)_2$·(E)-**1**$^-$ is not further considered.

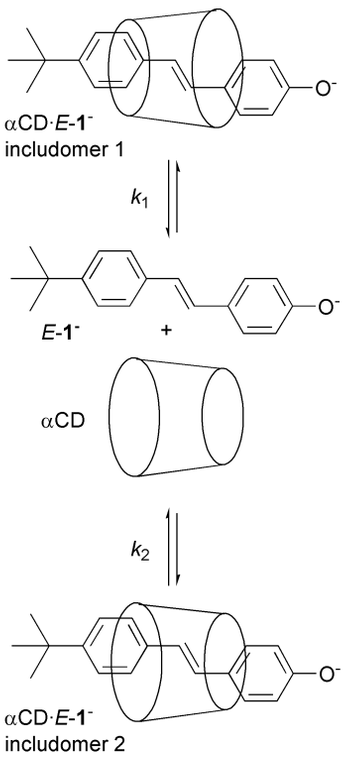

Scheme 2

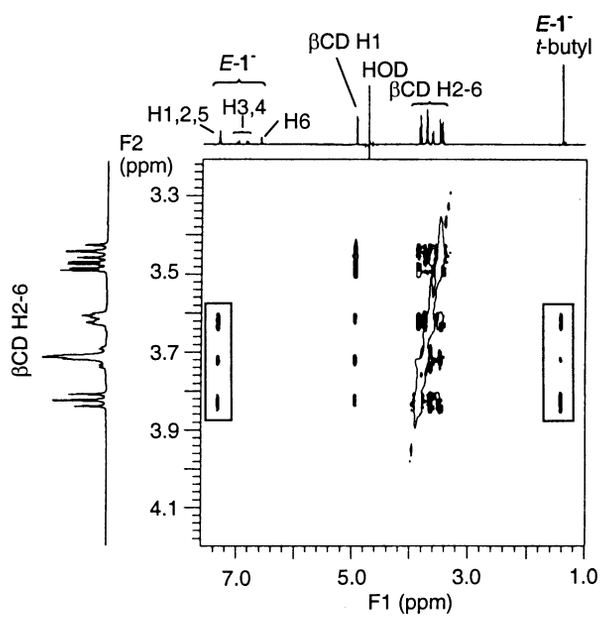

Fig. 3 ^{1}H 600 MHz ROESY NMR spectrum recorded at 298 K of a D_2O solution in which total [βCD], [(*E*)-**1**$^-$] and [NaOD] = 0.016, 0.015 and 0.15 mol dm^{-3}, respectively. The cross-peaks enclosed in the rectangles arise from dipolar interactions between the protons indicated on the F1 and F2 axes.

βCD·(*E*)-**1**$^-$ (Fig. 3). The βCD resonances are also better resolved than those of αCD in αCD·(*E*)-**1**$^-$ (Fig. 2). These differences indicate that the small size of αCD inhibits complexation of the *tert*-butyl end of (*E*)-**1**$^-$ to give two αCD·(*E*)-**1**$^-$ includomers (Scheme 2) and also slows their isomerization. The occurrence of cross-peaks arising from the *tert*-butyl protons and the H1 and H2 protons of (*E*)-**1**$^-$ but not from H3, H4 and H6 (and probably not from H5 although its resonance is too close to those of H1 and H2 to be certain) suggests that a dominant includomer of βCD·(*E*)-**1**$^-$ has the larger βCD annulus positioned over the *tert*-butyl end of (*E*)-**1**$^-$. In principle the two possible orientations of βCD could give two such includomers, but the sharpness of the resonances suggests that either these are in fast exchange or one dominates and is in slow exchange with the minor includomer which is below the level of detection.

Dynamic NMR studies of the αCD·(*E*)-1$^-$ complex

At 298 K, the one dimensional 600 MHz ^{1}H NMR spectrum of αCD·(*E*)-**1**$^-$ shows two singlets in a 1.00 : 0.85 area ratio arising from the *tert*-butyl protons of (*E*)-**1**$^-$ and most of the aromatic resonances of (*E*)-**1**$^-$ are split into two doublets. On increasing the temperature these singlets coalesce (Figs 4 and S2 †) consistent with (*E*)-**1**$^-$ exchanging between the two magnetic environments of the includomers shown in Scheme 2. Complete lineshape analysis[8,9] yields the exchange parameters: k_1(298 K) = 12.3 ± 0.6 s^{-1}, $\Delta H_1^{\ddagger}$ = 94.3 ± 4.7 kJ mol^{-1}, $\Delta S_1^{\ddagger}$ = 92.0 ± 5.0 J K^{-1} mol^{-1}, k_2(298 K) = 10.7 ± 0.5 s^{-1}, $\Delta H_2^{\ddagger}$ = 93.1 ± 4.7 kJ mol^{-1}, $\Delta S_2^{\ddagger}$ = 87.3 ± 5.0 J K^{-1} mol^{-1}, where the subscripts 1 and 2 refer to the lesser and more populated magnetic environments, respectively. The possibility of the (*E*)-**1**$^-$ coalescence phenomenon arising from exchange between complexed (*E*)-**1**$^-$ and free (*E*)-**1**$^-$ is excluded by the latter being of much too low a solubility to generate either of the *tert*-butyl resonances. Accordingly, the coalescence phenomenon is attributed to interchange of the two includomers of αCD·(*E*)-**1**$^-$ (Scheme 2) although it is not possible to assign the resonances to specific includomers.

As the ^{1}H ROESY NMR data discussed above indicate that αCD has difficulty in encompassing the *tert*-butyl group, dissociation of αCD·(*E*)-**1**$^-$ by passage of αCD over the phenoxy

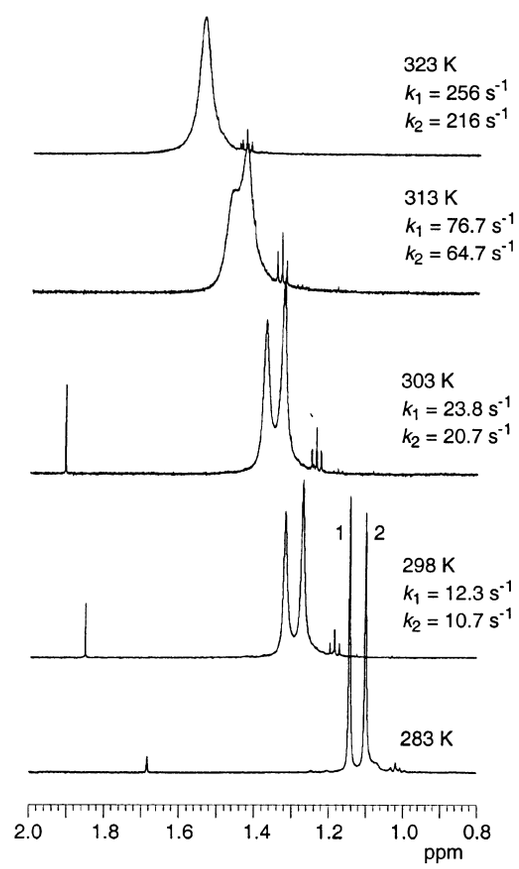

Fig. 4 Representative variable temperature ^{1}H NMR (600 MHz) spectra of the *tert*-butyl protons of (*E*)-**1**$^-$ in αCD·(*E*)-**1**$^-$ showing the derived rate constants k_1 and k_2 (the spectra are not plotted to a constant vertical scale). For the spectra not shown, k_1 = 45.3 s^{-1} and k_2 = 38.1 s^{-1} at 308 K, k_1 = 146 s^{-1} and k_2 = 123 s^{-1} at 318 K. The error in each rate constant is ±5%. The solution was made up in D_2O with total [αCD], [(*E*)-**1**$^-$] and [NaOD] = 0.010, 0.0034 and 0.15 mol dm^{-3}, respectively.

end of (*E*)-**1**$^-$ is probably the dominant isomerization mechanism for the includomers. The alternative associative mechanism proceeding *via* a transient (αCD)$_2$·(*E*)-**1**$^-$ complex appears less likely because of this steric hindrance. The positive $\Delta S_1^‡$ and $\Delta S_2^‡$ are consistent with a decrease in order which may indicate a partial dissociation of αCD·(*E*)-**1**$^-$ into its two components. It has been estimated that if all motions of the CD host and the guest species ceased on going from the free states to the complexed state an entropy change of −209 to −251 J K^{-1} mol^{-1} would result,[10] on which basis the reverse process would be characterised by a positive entropy change of similar magnitude. As it is unlikely that such a complete cessation of motion occurs in αCD·(*E*)-**1**$^-$, this is an upper limit for the magnitude of $\Delta S_1^‡$ and $\Delta S_2^‡$ for the includomer interconversion. In addition, hydration changes in both the αCD and (*E*)-**1**$^-$ components will occur as the transition state is approached, particularly for the entry of water into the αCD annulus as it is partly or completely vacated by (*E*)-**1**$^-$. Some change in hydration of the (*E*)-**1**$^-$ phenoxy group may also occur and both hydration changes should make a negative contribution to $\Delta S_1^‡$ and $\Delta S_2^‡$.

A comparison may be made between the αCD·(*E*)-**1**$^-$ data and those for the decomplexation of αCD·**5**$^-$, where **5**$^-$ is 4-(4-hydroxy-3,5-dimethylphenylazo)benzenesulfonate which is similar in size and shape to (*E*)-**1**$^-$.[11] This decomplexation occurs in two steps for which k(298 K) = 13.3 s^{-1}, $\Delta H^‡$ = 44.6 kJ mol^{-1}, $\Delta S^‡$ = −73.9 J K^{-1} mol^{-1} and $\Delta V^‡$ = −12.6 cm^3 mol^{-1} for the fast decomplexation step and k(298 K) = 0.22 s^{-1}, $\Delta H^‡$ = 47.5 kJ mol^{-1}, $\Delta S^‡$ = −98.3 J K^{-1} mol^{-1} and $\Delta V^‡$ = −16.1 cm^3 mol^{-1} for the slow decomplexation step and analogous data are reported for similar substituted azobenzene guests.[11] The decomplexation of αCD·(*E*)-**1**$^-$ may also proceed in two steps where the slower step is that characterized by ^{1}H NMR. A comparison with the parameters for the slower decomplexation step for αCD·**5**$^-$ shows that k(298 K) for αCD·(*E*)-**1**$^-$ is fifty times greater, $\Delta H^‡$ is larger by a factor of 2 and $\Delta S^‡$ is of a similar size but opposite in sign. The most obvious differences between the two complexes are that (*E*)-**1**$^-$ is very hydrophobic with only a phenoxy group to hydrogen bond with water whereas **5**$^-$ incorporates a diazo function, a phenolic hydroxy group and a sulfonate group, all of which are strongly hydrated. Thus, $\Delta S^‡$ for αCD·**5**$^-$ probably incorporates greater negative entropic contributions from hydration changes accompanying decomplexation than does that for αCD·(*E*)-**1**$^-$ which may explain the different signs of the $\Delta S^‡$ characterizing the two systems. A greater participation of water in the approach to the transition state may offset some of the enthalpy required to disrupt secondary bonding between αCD and **5**$^-$ in αCD·**5**$^-$ and thereby lower the overall $\Delta H^‡$ by comparison with that for the isomerization of αCD·(*E*) -**1**$^-$.

NMR studies of the complexation of (*E*)-1$^-$ and (*Z*)-1$^-$ by 2

Evidence for the formation of **2**·(*E*)-**1**$^-$ and **2**·(*Z*)-**1**$^-$ is provided by ^{1}H ROESY NMR spectroscopy which shows strong cross-peaks arising from dipolar interactions of the *tert*-butyl and the H1, H2, H5 and H6 protons of (*E*)-**1**$^-$ with the CD component H3, H5 and H6 protons of **2** as seen in Fig. 5. At 298 K the resonances of (*E*)-**1**$^-$ in **2**·(*E*)-**1**$^-$ are broadened consistent with the rate of either a rotational or a shuttling motion of (*E*)-**1**$^-$ within **2**·(*E*)-**1**$^-$ occurring within the intermediate ^{1}H NMR timescale. (As for αCD·(*E*)-**1**$^-$, resonance coalescence arising from exchange between complexed (*E*)-**1**$^-$ and free (*E*)-**1**$^-$ is ruled out by the latter being insufficiently soluble in water.) The intermediate rate of the motion of (*E*)-**1**$^-$ in **2**·(*E*)-**1**$^-$ appears to arise from the close fit of the αCD component annulus of **2** to (*E*)-**1**$^-$ and is consistent with no broadening of the (*E*)-**1**$^-$ resonances of **3**·(*E*)-**1**$^-$ occurring because the two βCD components of **3**$^-$ render it more commodious and allow more rapid motion of (*E*)-**1**$^-$.

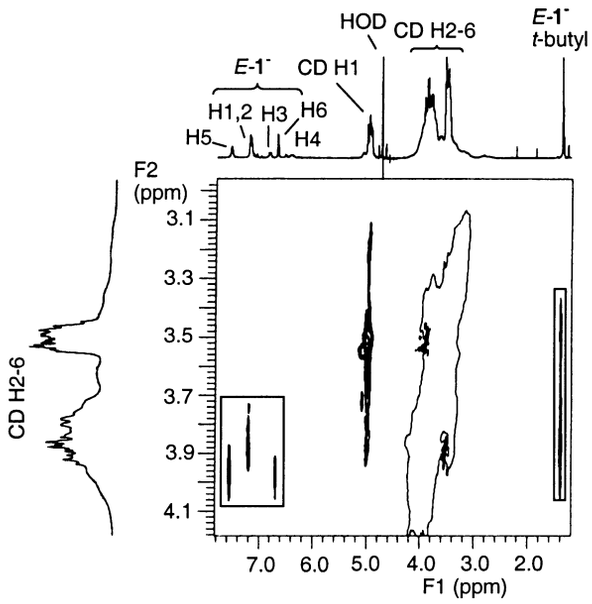

Fig. 5 ^{1}H 600 MHz ROESY NMR spectrum recorded at 298 K of a D_2O solution in which total [**2**], [(*E*)-**1**$^-$] and [NaOD] = 0.016, 0.015 and 0.15 mol dm^{-3}, respectively. The cross-peaks enclosed in the rectangles arise from dipolar interactions between the protons indicated on the F1 and F2 axes.

After exposure of the **2**·(*E*)-**1**$^-$ solution to sunlight for 2 h in a Pyrex vessel, during which time changes in its UV-visible spectrum indicated complete isomerization to **2**·(*Z*)-**1**$^-$, strong cross-peaks arising from the interaction of the *tert*-butyl and H1 and H2 protons of (*Z*)-**1**$^-$ with the CD component protons of **2** were observed in its ^{1}H ROESY NMR spectrum, but cross-peaks attributable to H5 and H6 of (*Z*)-**1**$^-$ were absent (Fig. 6). This is consistent with (*Z*)-**1**$^-$ occupying only one component annulus in **2**·(*Z*)-**1**$^-$. On the basis of the *tert*-butyl cross-peaks observed for both (*E*)-**1**$^-$ and (*Z*)-**1**$^-$ in **2**·(*E*)-**1**$^-$ and **2**·Z-**1**$^-$, in contrast to their absence from the ^{1}H ROESY NMR spectrum of αCD·(*E*)-**1**$^-$, and their presence in the ^{1}H ROESY NMR spectrum of βCD·(*E*)-**1**$^-$, it appears that the *tert*-butyl groups of (*E*)-**1**$^-$ and (*Z*)-**1**$^-$ are probably positioned in the βCD component annulus of **2** as shown for **2**·(*E*)-**1**$^-$ and **2**·(*Z*)-**1**$^-$ in

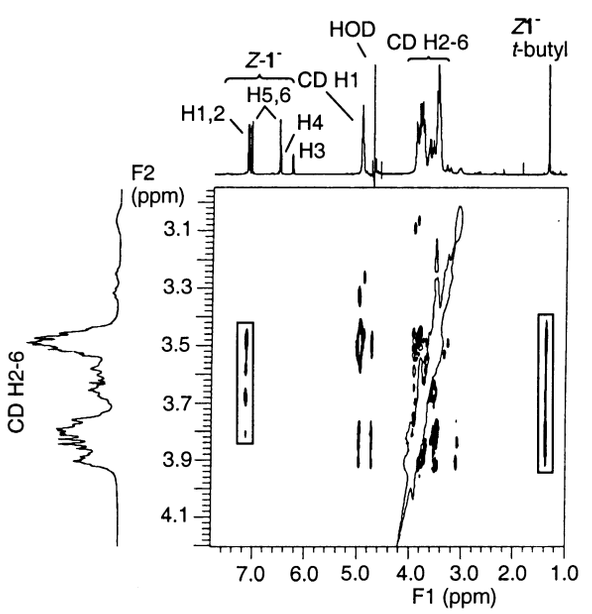

Fig. 6 ^{1}H 600 MHz ROESY NMR spectrum recorded at 298 K of a D_2O solution in which total [**2**], [(*Z*)-**1**$^-$] and [NaOD] = 0.016, 0.015 and 0.15 mol dm^{-3}, respectively. The cross-peaks enclosed in the rectangles arise from dipolar interactions between the protons indicated on the F1 and F2 axes.

Scheme 3. (While subsequent discussion is based on the includomers shown in Scheme 3, the existence of a minor includomer of each complex in which the *tert*-butyl groups of (*E*)-**1**$^-$ and (*Z*)-**1**$^-$ are positioned in the αCD component annulus of **2** cannot be excluded.) The (*Z*)-**1**$^-$ resonances of **2**·(*Z*)-**1**$^-$ are sharper than those of (*E*)-**1**$^-$ in **2**·(*E*)-**1**$^-$ consistent with the motion of (*Z*)-**1**$^-$ in the βCD component annulus being less impeded by comparison with that of (*E*)-**1**$^-$ which is complexed by both CD component annuli in **2**·(*E*)-**1**$^-$.

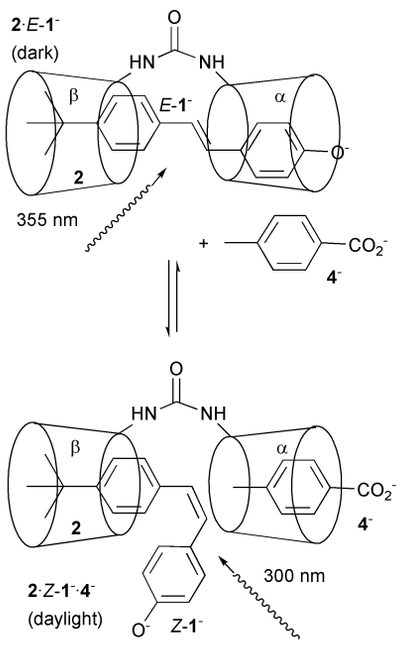

Scheme 3 Photoisomerization of **2**·(*E*)-**1**$^-$ and **2**·(*Z*)-**1**$^-$, the reverse thermal isomerization in the dark and the single irradiation wavelengths favouring **2**·(*E*)-**1**$^-$ and **2**·(*Z*)-**1**$^-$. The vacated αCD component annulus may be occupied by 4-methylbenzoate, **4**$^-$, to form **2**·(*Z*)-**1**$^-$·**4**$^-$.

When 4-methylbenzoate, **4**$^-$, is present in solution, the ^{1}H ROESY NMR spectrum of **2**·(*E*)-**1**$^-$ shows no cross-peaks attributable to interactions between the protons of **4**$^-$ and **2** (Fig. 7 and expanded in Fig. S3†), whereas in the presence of **2**·(*Z*)-**1**$^-$ a strong cross-peak is observed for the methyl protons

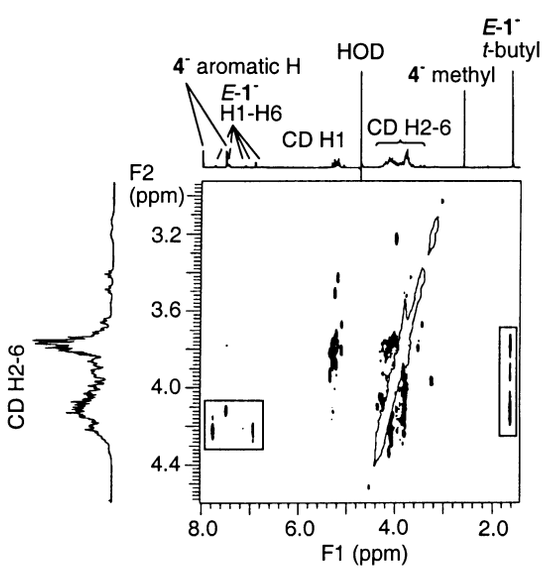

Fig. 7 ^{1}H 600 MHz ROESY NMR spectrum recorded at 298 K of a D_2O solution in which total [**2**], [(*E*)-**1**$^-$], [**4**$^-$] and [NaOD] = 0.016, 0.015, 0.022 and 0.15 mol dm^{-3}, respectively. The cross-peaks enclosed in the rectangles arise from dipolar interactions between the protons indicated on the F1 and F2 axes.

of **4**$^-$ and a weaker cross-peak for the aromatic protons (Fig. 8 and expanded in Fig. S4†) consistent with the formation of the **2**·(*Z*)-**1**$^-$·**4**$^-$ ternary complex as shown in Scheme 3. (Analogous cross-peaks are similarly absent and present from the ^{1}H ROESY NMR spectra of **2**·(*E*)-**1**$^-$ and **2**·(*Z*)-**1**$^-$, respectively, in the presence of 4-methylphenolate and 4-methylsulfonate.) Thus, it appears that **4**$^-$ occupies the αCD component annulus of **2** vacated by the phenoxy end of (*Z*)-**1**$^-$ in **2**·(*Z*)-**1**$^-$·**4**$^-$. The cross-peak arising from **4**$^-$ disappears and the spectrum reverts to that of **2**·(*E*)-**1**$^-$ and **4**$^-$ when **2**·(*E*)-**1**$^-$ reforms through the thermal isomerization path in the dark. The interconversion of these complexes constitute the operation of a molecular device which may be controlled by either alternating photoisomerization of (*E*)-**1**$^-$ and thermal isomerization of (*Z*)-**1**$^-$ or by photoisomerization of (*E*)-**1**$^-$ and (*Z*)-**1**$^-$ alone, although in the latter case this amounts to the attainment of wavelength dependent photostationary states in which the proportions of **2**·(*Z*)-**1**$^-$·**4**$^-$ and **2**·(*E*)-**1**$^-$ and **4**$^-$ differ. The analogous 4-methylphenolate and 4-methylphenylsulfonate systems behave similarly.

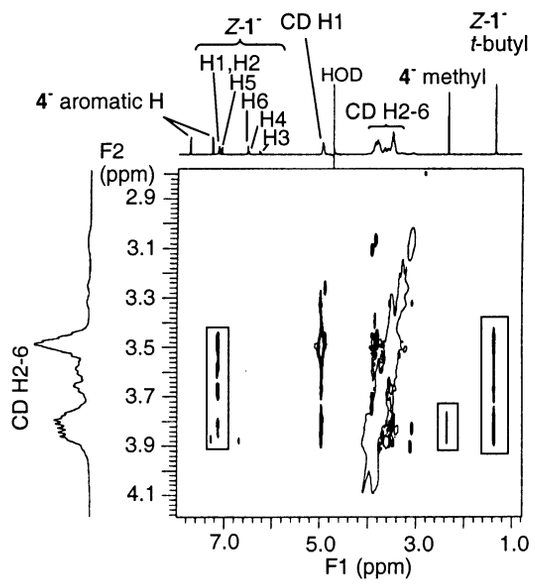

Fig. 8 ^{1}H 600 MHz ROESY NMR spectrum recorded at 298 K of the solution from Fig. 7 after a 2 h exposure to daylight to give **2**·(*Z*)-**1**$^-$·**4**$^-$, **2**·(*Z*)-**1**$^-$ and **4**$^-$. The cross-peaks enclosed in the rectangles arise from dipolar interactions between the protons indicated on the F1 and F2 axes.

The complexation of **4**$^-$ in **2**·(*Z*)-**1**$^-$·**4**$^-$, but not in **2**·(*E*)-**1**$^-$, represents a fine balance between the greater complexing abilities of (*Z*)-**1**$^-$ and (*E*)-**1**$^-$ and the lesser complexing ability of **4**$^-$. A change in this balance occurs with more strongly complexing adamantane-1-carboxylate, **6**$^-$. In contrast to **2**·(*E*)-**1**$^-$ and **4**$^-$, which do not detectably interact in solution, the interaction between **2** and **6**$^-$ in a solution where [**2**], [(*E*)-**1**$^-$], [**6**$^-$] and [NaOD] = 0.016, 0.015, 0.022 and 0.15 mol dm^{-3}, respectively, produced strong ^{1}H ROESY NMR cross-peaks and those arising from **2**·(*E*)-**1**$^-$ are decreased in intensity but unchanged in character. This is most simply explained in terms of a competitive equilibrium where the major complexes are **2**·(*E*)-**1**$^-$ and **2**·**6**$^-$. Complexation constants $K = 1.8 \times 10^4$ and 1.84×10^4 dm^3 mol^{-1} are reported[12,13] for the complexation of **6**$^-$ and 4-*tert*-butylbenzoate, respectively, by βCD on which basis significant competition between **6**$^-$ and the *tert*-butyl end of (*E*)-**1**$^-$ for occupancy of the βCD component annulus of **2** is expected. (Complexation of **4**$^-$ by αCD is characterized by K = 110 dm^3 mol^{-1} consistent with **4**$^-$ not competing with (*E*)-**1**$^-$ for occupancy of the βCD component annulus of **2**.[12]) Because of its large size, **6**$^-$ is complexed less strongly by αCD (K = 140 dm^3 mol^{-1})[14] and is therefore less likely to compete with (*E*)-**1**$^-$ and

(*Z*)-**1**$^-$ for occupancy of the αCD component annulus of **2**. The ^{1}H ROESY NMR spectrum of a solution in which [**2**], [(*Z*)-**1**$^-$], [**6**$^-$] and [NaOD] = 0.016, 0.015, 0.022 and 0.15 mol dm^{-3}, respectively, produced strong cross-peaks arising from dipolar interactions between **2** and (*Z*)-**1**$^-$ and between **2** and **6**$^-$ which may also be explained in terms of the competitive formation of **2**·(*Z*)-**1**$^-$ and **2**·**6**$^-$. The possibility of forming the ternary complexes **2**·(*E*)-**1**$^-$·**6**$^-$ and **2**·(*Z*)-**1**$^-$·**6**$^-$ also exists.

NMR studies of the complexation of 1$^-$ by 3

Evidence for the formation of **3**·(*E*)-**1**$^-$ and **3**·(*Z*)-**1**$^-$ is provided by ^{1}H ROESY NMR spectroscopy. For a solution in which total [**3**], [(*E*)-**1**$^-$] and [NaOD] = 0.016, 0.015 and 0.15 mol dm^{-3}, respectively, strong cross-peaks arising from dipolar interactions of the *tert*-butyl and the H1, H2, H5 and H6 protons of (*E*)-**1**$^-$ with the H3, H5 and H6 protons of the annuli of the βCD components of **3** in **3**·(*E*)-**1**$^-$ are seen (Fig. 9). This is also the case when (*E*)-**1**$^-$ is isomerized to (*Z*)-**1**$^-$ (Fig. 10) consistent with both of the two βCD components of **3**·(*Z*)-**1**$^-$ being occupied and also with the annuli of the two βCD components together being of sufficient volume to accommodate (*Z*)-**1**$^-$, unlike the situation with **2**·(*Z*)-**1**$^-$.

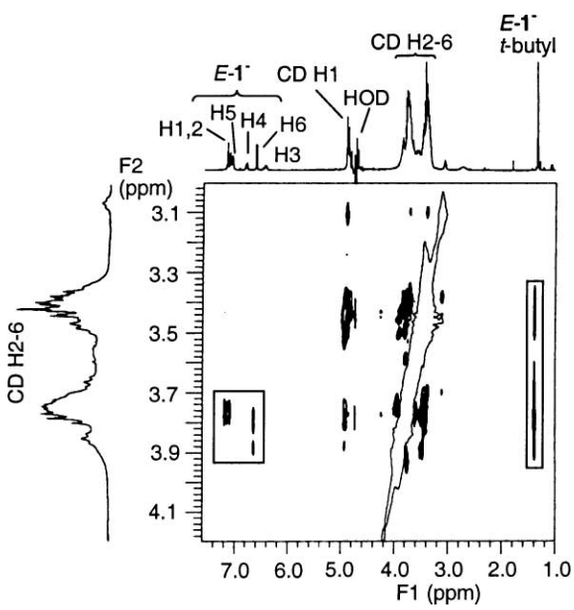

Fig. 9 ^{1}H 600 MHz ROESY NMR spectrum recorded at 298 K of a D_2O solution in which total [**3**], [(*E*)-**1**$^-$] and [NaOD] = 0.016, 0.015 and 0.15 mol dm^{-3}, respectively. The cross-peaks enclosed in the rectangles arise from dipolar interactions between the protons indicated on the F1 and F2 axes.

No cross-peaks arising from the simultaneous complexation of **4**$^-$ in the presence of **3**·(*E*)-**1**$^-$ were observed. However, cross-peaks arising from the interaction of both the aromatic protons of the phenolate end of (*Z*)-**1**$^-$ and **4**$^-$ with a βCD component annulus of **3** were observed for a solution of 0.016, 0.015 and 0.022 mol dm^{-3} in **3**, (*Z*)-**1**$^-$ and **4**$^-$, respectively, in 0.15 mol dm^{-3} NaOD consistent with **3**·(*Z*)-**1**$^-$ existing in an equilibrium between an includomer in which both βCD component annuli are occupied by (*Z*)-**1**$^-$ and one in which only one βCD component annulus is occupied by the *tert*-butyl end of (*Z*)-**1**$^-$ and the other βCD component annulus is empty. It is this vacant annulus which may be occupied by **4**$^-$ to give **3**·Z-**1**$^-$·**4**$^-$.

Conclusion

The effect of the smaller αCD annular size on complexation processes is shown by the slowing of the isomerization of αCD·(*E*)-**1**$^-$ to within the NMR kinetic timescale and the exclusion

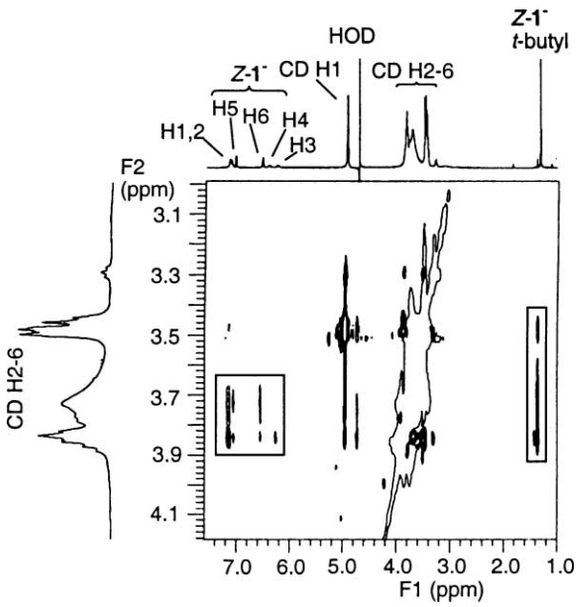

Fig. 10 ^{1}H 600 MHz ROESY NMR spectrum recorded at 298 K of a D_2O solution in which total [**3**], [(*Z*)-**1**$^-$] and [NaOD] = 0.016, 0.015 and 0.15 mol dm^{-3}, respectively. The cross-peaks enclosed in the rectangles arise from dipolar interactions between the protons indicated on the F1 and F2 axes.

of the *tert*-butyl group of (*E*)-**1**$^-$ from the αCD annulus. In contrast, βCD·(*E*)-**1**$^-$ allows entry of the *tert*-butyl group of (*E*)-**1**$^-$ into the larger βCD annulus and either a dominant βCD·(*E*)-**1**$^-$ includomer to be formed or isomerization between βCD·(*E*)-**1**$^-$ includomers to occur at a rate in the fast exchange limit of the NMR timescale. The effect of the photoisomerization of (*E*)-**1**$^-$ and (*Z*)-**1**$^-$ is amplified in **2**·(*E*)-**1**$^-$ and **2**·(*Z*)-**1**$^-$ through the occupancy of both the αCD and the βCD component annuli in **2**·(*E*)-**1**$^-$ whereas the vacating of the βCD annulus in **2**·(*Z*)-**1**$^-$ allows 4-methylbenzoate, **4**$^-$, 4-methylphenolate and 4-methylphenylsulfonate to enter it to form a ternary complex exemplified by **2**·(*Z*)-**1**$^-$·**4**$^-$. Thus, **2**·(*E*)-**1**$^-$ and **2**·(*Z*)-**1**$^-$ represent two states of a simple photo-controlled molecular assembly in which the effects of stilbene isomerization is amplified by its environment in **2**. While the **3**·(*E*)-**1**$^-$ and **3**·(*Z*)-**1**$^-$ includomers behave similarly to their **2** analogues, their interactions appear to be more flexible because of the greater combined size of the two βCD component annuli of **3**.

Experimental

General

^{1}H (300 MHz) and ^{13}C (75.5 MHz) NMR spectra were run in $CDCl_3$ on a Varian Gemini 300 spectrometer and were referenced either against internal TMS or the proton impurity ^{13}C multiplet (δ = 39.5 ppm). ^{1}H (600 MHz) NMR spectra were run on an Inova 600 spectrometer. The ^{1}H 2D-ROESY NMR spectra were recorded using a standard pulse sequence with a mixing time of 0.3 seconds. All of the spectra appearing in the Figures were referenced to the HOD resonance at δ = 4.72 ppm. All other spectra were referenced against external trimethylsilylpropiosulfonic acid. The lineshape analysis of the coalescence of the *tert*-butyl resonances of the αCD·(*E*)-**1**$^-$ includomers was carried out using the program DAVNMR.[9] The mole fractions of each includomer and their chemical shift difference showed no significant variation in the slow exchange region over the temperature range 278–298 K and this was assumed to be the case in the range 298–323 K over which lineshape analysis was carried out. The slight narrowing of the includomer resonances occurring in the temperature range 278–288 K was extrapolated into the coalescence temperature range

to give the non-exchange modified T_2 for the lineshape analysis. The best fit of the calculated lineshape to the experimental lineshape was obtained through minimizing the mean of the squares of the residual difference between the two.

MALDI-TOF mass spectrometry was carried out at the Research School of Chemistry at the Australian National University, Canberra, ACT. Electrospray mass spectrometry (ES-MS) and fast atom bombardment mass spectrometry (FAB-MS) were carried out at the University of Adelaide. Samples for ES-MS were dissolved in water for injection. Infrared spectra were recorded on an ATI Mattson Genesis FT-IR. The abbreviations strong (s), medium (m), weak (w) and broad (b) are used for reporting the intensity of the bands observed. UV/vis spectra were recorded on a Cary 300 Bio spectrophotometer. Irradiation of solutions of the (*E*)-**1**$^-$ and (*Z*)-**1**$^-$ complexes were carried out in a quartz cuvette in a LS50B fluorimeter. Elemental analyses were performed by the Microanalytical Service of the Chemistry Department, University of Otago, Dunedin, New Zealand. Thin layer chromatography (TLC) was carried out on Kieselgel 60 F_{254} (Merck) on aluminium-backed sheets.

All reagents used were obtained from Aldrich and were not further purified before use, unless otherwise stated. β-Cyclodextrin was donated by Nihon Shokuhin Kako Co. Both αCD and βCD were dried by heating at 100 °C under reduced pressure for 18 hours. The linked CDs **2** and **3** were prepared by a literature procedure.[5] Pyridine and 1-methylpyrrolidin-2-one (NMP) were dried by distillation from calcium hydride. *N*,*N*-Dimethylformamide (DMF) and methanol were dried over molecular sieves.

Preparation of 4-*tert*-butyl-4′-methoxystilbene

(a) 4-*tert*-Butylbenzylbromide (0.451 g, 1.99 mmol) and triethyl phosphite (0.5 cm^3) were stirred at 120 °C for 12 hours. Excess triethyl phosphite was removed at reduced pressure to give diethyl (4-*tert*-butylbenzyl)phosphonate (quantitative yield). $\delta_H(CDCl_3)$ 7.20–7.29 (m, 4H, ArH), 3.94–4.05 (m, 4H, CH_3CH_2O), 3.11 (d, J = 21 Hz, 2H, CH_2–P), 1.30 (s, 9H, $C(CH_3)_3$), 1.24 (t, J = 6.8 Hz, CH_3CH_2O).

(b) Diethyl (4-*tert*-butylbenzyl)phosphonate (0.508 g, 1.79 mmol) was dissolved in dry THF (20 cm^3) and sodium hydride (0.067 g, 2.79 mmol) was added at 0 °C. Anisaldehyde (0.220 cm^3, 1.81 mmol) was added and the mixture was allowed to slowly warm up to room temperature. The mixture was stirred for 24 hours, followed by the addition of water (4 cm^3) and 1 mol dm^{-3} hydrochloric acid (5 cm^3). The organic layer was separated and the aqueous layer was extracted with ether (3 × 10 cm^3). The combined organic layers were washed with saturated ammonium bicarbonate (15 cm^3), dried (sodium sulfate), filtered and concentrated. Purification by flash column chromatography (30% ethyl acetate–hexane) gave the pure product as white crystals (0.287 g, 60 %), mp 179–181 °C; FAB-MS *m*/*z* 266 (M$^+$) [Found: C, 85.60; H, 8.01%. Calc. for $C_{19}H_{22}O$: C, 85.67; H, 8.32%)]; $\delta_H(CDCl_3)$ 7.45 (d, J = 9.0 Hz, 2H, ArH5), 7.43 (δ_A), 7.37 (δ_B) (AB q, J_{AB} = 9.0 Hz, 4H, ArH1,2), 7.04 (d, J = 16.6 Hz, 1H, C=C–H), 6.96 (d, J = 16.6 Hz, 1H, C=C–H), 6.90 (d, J = 9.0 Hz, 2H, ArH6), 3.83 (s, 3H, O–CH_3), 1.33 (s, 9H, $C(CH_3)_3$); $\delta_C(CDCl_3)$ 150.30, 134.84, 130.33, 127.56 (ArC); 127.41, 126.40 (C=C); 127.56, 125.94, 125.55, 114.06 (ArC); 55.31 (O–CH_3); 34.57 ($C(CH_3)_3$); 31.28 ($C(CH_3)_3$); ν_{max} (Nujol/cm^{-1}) 1602m (C=C), 1590w, 1511m (Ar), 969m (H–C=C–H), 833s (Ar).

Preparation of (*E*)-(4-*tert*-butyl-4′-hydroxystilbene), (*E*)-4H

Sodium hydride (0.242 g (60%), 6.05 mmol) was suspended in dry DMF (10 cm^3) and ethanethiol (0.250 cm^3, 3.01 mmol) was added dropwise at room temperature, followed by (*E*)-4-*tert*-butyl-4′-methoxystilbene (0.297 g, 1.11 mmol). The mixture was stirred at 100 °C for 5 hours then cooled to room temperature and quenched with 3 mol dm^{-3} hydrochloric acid. Ether (5 cm^3) was added, the organic layer was separated and the aqueous layer was extracted with more ether (2 × 5 cm^3). The combined organic layers were washed with 5% sodium hydroxide (3 × 5 cm^3) and brine (5 cm^3), dried (sodium sulfate) and concentrated. The crude material was purified by flash column chromatography (10%–25% ethyl acetate–hexane) to give the pure product as a white solid (0.231 g, 83%), mp 160–162 °C; FAB-MS *m*/*z* 252 (M$^+$) [Found: C, 83.70; H, 8.15%. Calc. for $(C_{18}H_{20}O)_3 \cdot H_2O$: C, 83.68; H, 8.06%]; $\delta_H(CDCl_3)$ 7.35–7.44 (m, 6H, ArH1,2,5), 7.02 (d, J = 16.5 Hz, 1H, C=CH), 6.94 (d, J = 16.5 Hz, 1H, C=CH), 6.82 (d, J = 8.4 Hz, 2H, ArH6), 4.86 (br s, 1H, OH), 1.33 (s, 9H, $C(CH_3)_3$); $\delta_C(CDCl_3)$ 155.02, 150.36, 134.78, 130.56, 127.78 (ArC); 127.33, 126.49 (C=C); 125.96, 125.56, 115.54 (ArC); 34.57 ($C(CH_3)_3$); 31.28 ($C(CH_3)_3$); ν_{max} (Nujol/cm^{-1}) 3150–3250b (O–H), 1607m (C=C), 1592m, 1510m (Ar), 1253m (O–H), 971m (H–C=C–H), 835s (Ar).

Preparation of (*Z*)-(4-*tert*-butyl-4′-hydroxystilbene), (*Z*)-4H

(*E*)-(4-*tert*-Butyl-4′-hydroxystilbene) (0.200 g, 0.794 mmol) was dissolved in deoxygenated methanol (15 cm^3), placed in a flask with a lightly greased stopper, and was exposed to sunlight for 24 hours. Solvent was removed under reduced pressure and the crude material was loaded onto a neutral alumina column and eluted with 30% ethyl acetate–hexane to give the pure (*Z*)-isomer as a viscous oil which solidified upon cooling (0.110 g, 55%), and the (*E*)-isomer was recovered (0.047 g, 24%); FAB-MS *m*/*z* 252 (M$^+$) [Found: C, 84.18; H, 8.58%. Calc. for $(C_{18}H_{20}O)_3 \cdot H_2O$ C, 83.68; H, 8.06%]; $\delta_H(CDCl_3)$ 7.20–7.27 (m, 4H, ArH1,2), 7.17 (d, J = 8.4 Hz, 2H, ArH5), 6.71 (d, J = 8.4 Hz, 2H, ArH6), 6.47 (br s, 2H, HC=CH), 4.80 (br s, 1H, OH), 1.29 (s, 9H, $C(CH_3)_3$); $\delta_C(CDCl_3)$ 154.82, 150.28, 134.71, 130.89, 130.61 (ArC); 129.10, 129.33 (C=C); 128.84, 125.42, 115.40 (ArC); 34.81 ($C(CH_3)_3$); 31.59 ($C(CH_3)_3$).

Acknowledgements

We thank the Australian Research Council for supporting this research, the University of Adelaide for awarding an Adelaide National Research Scholarship to J.S.L and to Nihon Shokhuin Kako Co for a gift of β-cyclodextrin.

References

1 C. J. Easton and S. F. Lincoln, *Modified Cyclodextrins, Scaffolds and Templates for Supramolecular Chemistry*, Imperial College Press, London, UK, 1999.
2 K. A. Connors, *Chem. Rev.*, 1997, **97**, 1325; H.-J. Schneider, F. Hacket and V. Rüdiger, *Chem. Rev.*, 1998, **98**, 1755; K. Harata, *Chem. Rev.*, 1998, **98**, 1803; M. V. Rekharsky and Y. Inoue K. Harata, *Chem. Rev.*, 1998, **98**, 1875.
3 V. Balzani, A. Credi, F. M. Raymo and J. F. Stoddart, *Angew. Chem., Int. Ed.*, 2000, **39**, 3348; V. Balzani, A. Credi, F. Marchioni and J. F. Stoddart, *Chem. Commun.*, 2001, 1860; T. Fujimoto, A. Nakamura, Y. Inoue, S. Sakata and T. Keneda, *Tetrahedron Lett.*, 2001, 7987; C. A. Stanier, S. J. Alderman, T. W. Claridge and H. L. Anderson, *Angew. Chem., Int. Ed.*, 2002, **41**, 1769; A. Mulder, A. Jukovic, L. N. Lucas, J. van Esch, B. L. Feringa, J. Huskens and D. N. Reinhoudt, *Chem. Commun.*, 2002, 2734.
4 D. H. Waldeck, *Chem. Rev.*, 1991, **91**, 415; H. Görner and H. J. Kuhn, *Adv. Photochem.*, 1995, **19**, 1.
5 M. M. Cieslinski, P. Clements, B. L. May, C. J. Easton and S. F. Lincoln, *J. Chem. Soc., Perkin Trans. 2*, 2002, 947 (in this reference the concentration scales of Fig 2a) and b) should read $10^3[\mathbf{1}]_{total}$/mol dm^{-3} and $10^3[\mathbf{2}]_{total}$/mol dm^{-3}, respectively.).
6 C. J. Easton, S. J. van Eyk, S. F. Lincoln, B. L. May, J. Papageorgiou and M. L. Williams, *Aust. J. Chem.*, 1997, **50**, 9.
7 W. Saenger, J. Jacob, K. Gessler, T. Steiner, D. Hoffmann, H. Sanbe, K. Koizumi, S. M. Smith and T. Takaha, *Chem. Rev.*, 1998, **98**, 1787.
8 S. F. Lincoln, *Prog. React. Kinet.*, 1977, **9**, 1.
9 Program DAVNMR, private communication from David Brittain, University of Adelaide, 2003.

10 I. Tabushi, Y.-I. Kiyosuke, T. Sugimoto and K. Yamamura, *J. Am. Chem. Soc.*, 1978, **100**, 916.
11 A. Abou-Hamdan, P. Bugnon, C. Saudan, P. G. Lye and A. E. Merbach, *J. Am. Chem. Soc.*, 2000, **122**, 592; C. Saudan, F. A. Dunand, A. Abou-Hamdan, P. Bugnon, P. G. Lye, S. F. Lincoln and A. E. Merbach, *J. Am. Chem. Soc.*, 2001, **123**, 10290.
12 M. R. Eftink, M. L. Andy, K. Bystrom, H. D. Perlmutter and D. S. Kristol, *J. Am. Chem. Soc.*, 1989, **111**, 6765.
13 T. Höfler and G. Wenz in *Proceedings of the Eighth International Conference on Cyclodextrins*, eds. J. Szejtli and L. Szente, Kluwer, Dordrecht, The Netherlands, 1996.
14 E. Brown, J. H. Coates, P. A. Duckworth, S. F. Lincoln, C. J. Easton and B. L. May, *J. Chem. Soc., Faraday Trans.*, 1993, **89**, 1035.